A three-component field study of the effect of the low-velocity layer on converted-wave seismic data

Dan Cieslewicz and Don C. Lawton

ABSTRACT

A field experiment was devised to study shear-wave attenuation in the low-velocity surface layer by burying three geophones at approximately 6m, 12m, and 18m depths, and placing one on the surface. The geophones collected data during the shooting of a regular dynamite-source three-component line. A frequency analysis of the regular and converted-wave reflections showed that P-S reflections were already substantially attenuated compared to P-P reflections even at a depth of 18m. No difference in attenuation was observed between the different geophone depths. Uphole interval velocity calculations, based on reflected arrivals, showed the presence of the water table between 12 and 18m depths. Above the water table, Vp/Vs was 2 to 3, while below the water table, Vp/Vs had a very large value of 10.7. The experiment should be repeated with geophones that preferably reach the top of the bedrock.

INTRODUCTION

The bandwidth of P-wave VSP has usually been found to be comparable to P-S VSP (e.g., Geis et al., 1990; Zhang et al., 1994). Since S-waves travel more slowly than P-waves, this implies that they have a shorter wavelength, which in turn results in P-S VSP sections having higher resolution than P-P VSP sections. Converted-wave sections from surface seismic data, however, usually have a considerably lower bandwidth compared to P-S VSP section (e.g. Zhang et al., 1994). Surface P-P sections do not have the same degree of attenuation compared to P-P VSP sections.

This reduction in bandwidth of the surface P-S data is due to a number of factors. Firstly, shear-waves attenuate faster in general compared to compressional waves of the same frequency due to their shorter wavelength. This means that S-waves have to complete more cycles than P-waves going an equivalent distance; as attenuation is a measure of energy loss per cycle, greater attenuation in the S-wave results. In addition, laboratory measurements (e.g. Toksöz et al., 1978) indicate that brine and water-saturated rock is in general more attenuative (has lower Q) for S-waves than for P-waves. Another important factor is that in surface seismic data, the waves pass through the low-velocity layer before being recorded, whereas in VSP data they do not. The reduction in bandwidth seen in converted-wave reflections may therefore be due to high shear-wave attenuation in the low-velocity layer.

The purpose of the field test was to determine if shear-wave attenuation could be detected through the low-velocity layer and, if possible, estimate a shear-wave attenuation constant (Q) for the layer. The low-velocity layer was studied by burying 3-component geophones to different depths in the overburden and examining the frequency content of upgoing converted-wave reflections. If a value for shear-wave Q can be determined, then it is possible to design inverse Q filters that could recover at least part of the lost bandwidth. This would obviously improve the quality and resolution of the converted-wave data. Also, there may exist a particularly attenuative zone near the surface which can be avoided by burying the geophones to a relatively shallow depth.

This experiment also enabled accurate calculations of short interval uphole P and S-wave interval velocities, which should improve our understanding of this important but often underappreciated layer.

DESCRIPTION OF EXPERIMENT

The experiment coincided with the shooting of a 3C-2D seismic line in southern Alberta by a CREWES sponsor. The source was 4kg of dynamite detonated at a depth of 18m, with a nominal shot interval of 40m. The receiver interval for the line was 20m, with a maximum source-receiver offset of 1300m. Topographic relief in the area was very low (<5m) and surficial geology was mainly recessional moraine composed of unsorted silt, sand and gravel (Westgate, 1963).

The experiment was performed at three separate locations on the line: group 1 was located near the eastern end of the line, group 2 in the central part of the line, and group 3 near the western end of the line. The groups were placed at receiver stations of the 2D seismic line, and spaced far enough apart so as to have no shot points in common. At each location, a drill rig augured three vertical holes to different depths, as detailed in Table 1 (for completeness, the surface geophone location is also included). Auguring was facilitated by simultaneously injecting water into the hole.

	Group 1	Group 2	Group 3
Depth 1	0	0	0
Depth 2	6	6	5
Depth 3	12	10	11
Depth 4	18	18	17

Table 1. Geophone depths (in meters) of the different groups.

The geophones used were OYO Geospace three-component phones. The ones that were buried were first placed on a planting pole, aligned visually so that the radial channel paralleled the 2-D line, and then lowered down the hole. Several planting poles had to be linked together before the phones reached bottom. Pole-planters generally encountered 1-3m of thick mud before achieving a reasonably firm plant at the bottom of the hole, which was obtained by both planters leaning their full weight on the poles. As anticipated, these geophones could not be recovered. Hole locations and depths were marked with stakes. The surface geophones were planted in a 15 cm deep hole, leveled and aligned in the usual fashion, and then covered to reduce wind noise.

The contractor brought the buried phones up live when the receiver location became part of the active spread. Three seconds of data were collected at a sample rate of 2ms, which was stored by the contractor as a separate line. Later the data were sifted off and delivered to CREWES.

PROCESSING

The processing steps for data presented in this report are outlined in Figure 1. The entire dataset consisted of 36 common receiver gathers (3 groups×4 receivers per group×3 channels per receiver), each containing an average of 65 traces. For display purposes, padded traces and variable trace spacing are used, as field operations required that some shot stations had to be skipped. Usually fold was maintained by halving the shot interval around these areas.

Various data rotations were attempted but were found to at best only nominally increase the amplitude of the converted-wave reflections on the radial channel. This indicates that the geophones did not rotate greatly from their initial orientation as they were lowered down the holes.

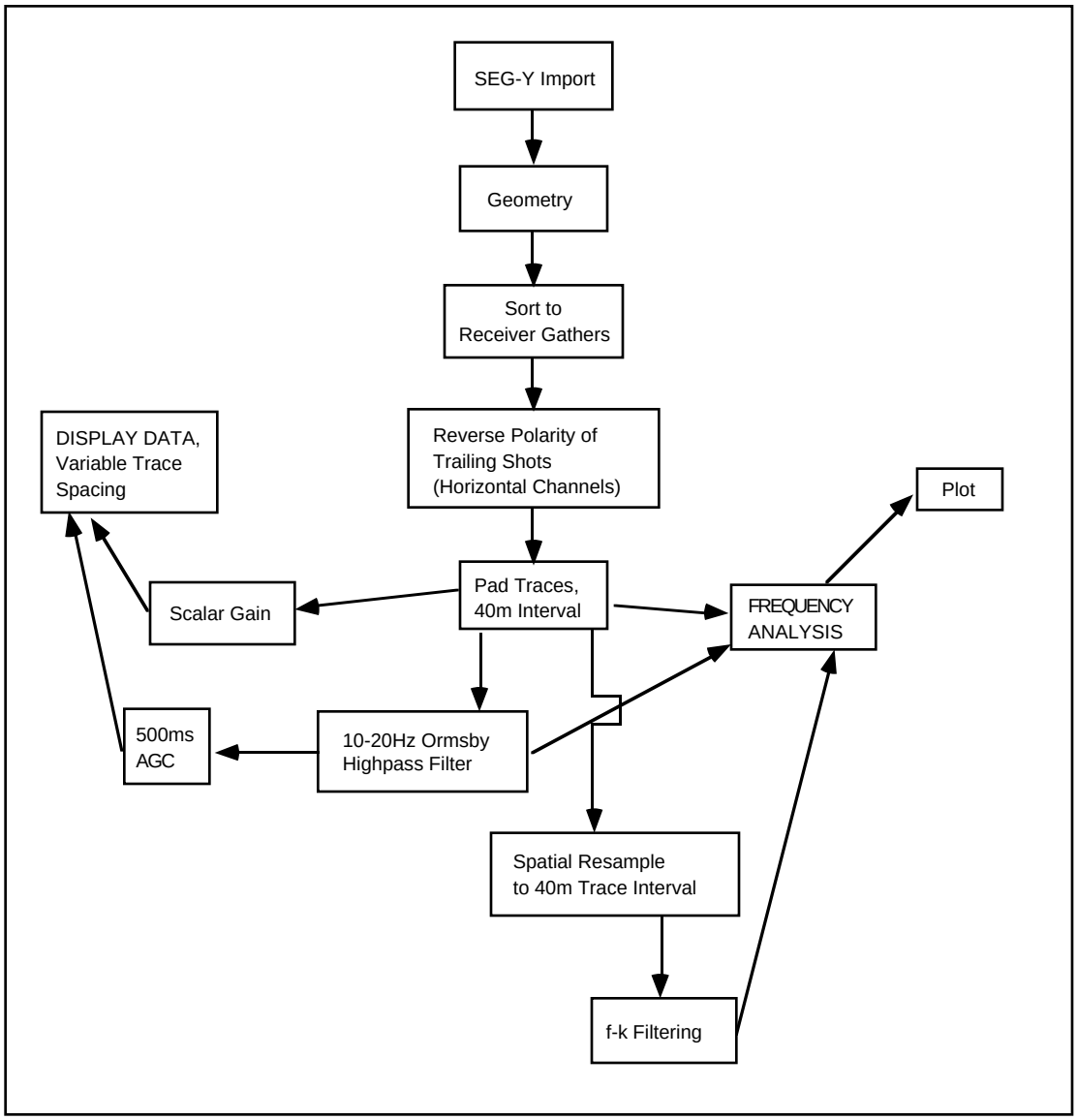

Figure 1. Processing steps for data presented in this paper

ANALYSIS OF DATA

Figure 2 shows the raw data for all channels of group 1. Only a single scalar gain was used for all traces, so relative amplitudes within each gather and between gathers has been preserved. Ground roll is clearly prominent at all receiver depths, and decays with depth. Refracted arrivals have their greatest amplitude in the surface receiver gather, a clear demonstration of the free-surface effect.

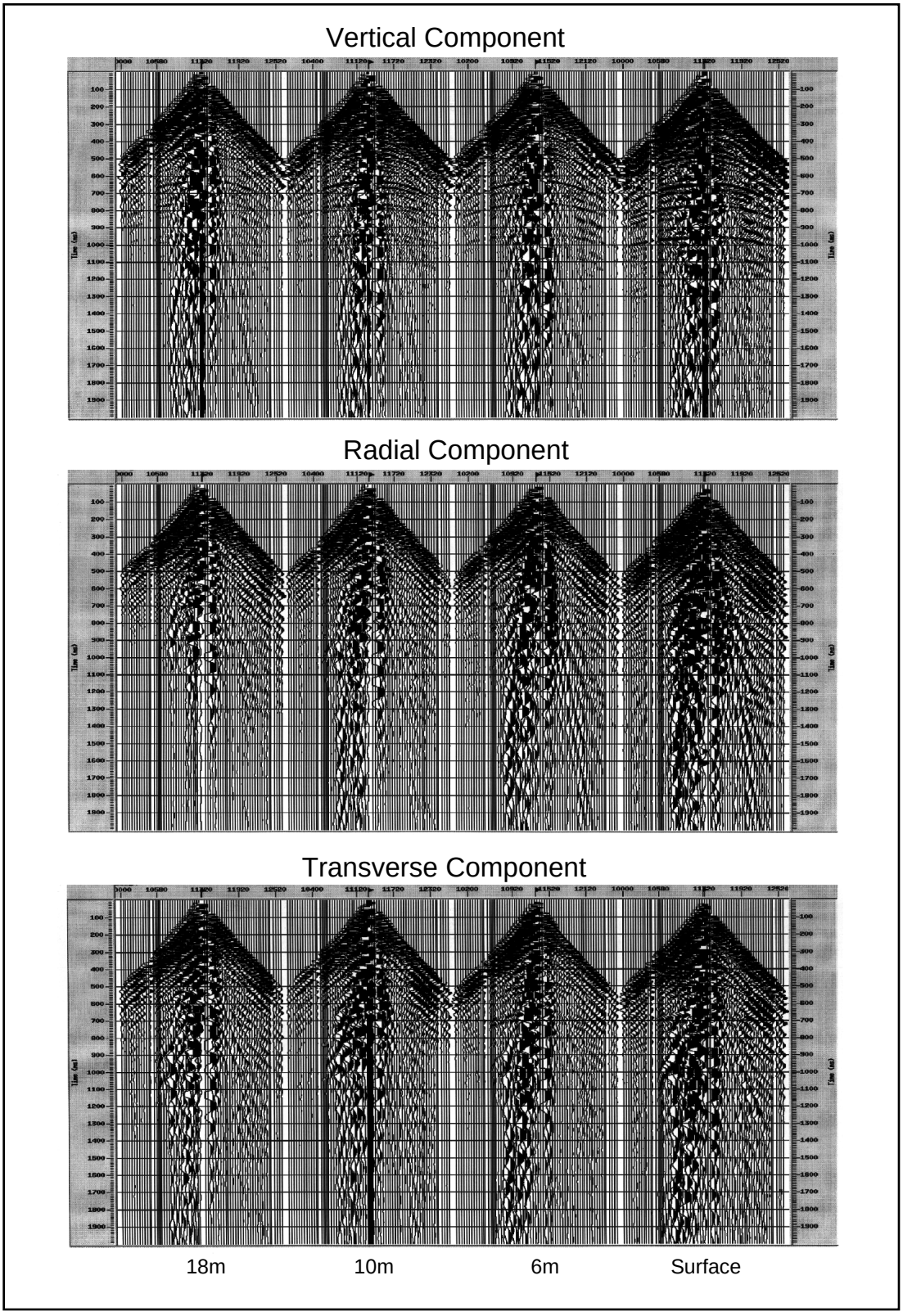

Figure 2. Group 2, raw traces, all components and depths.

To reduce ground roll and enhance reflections, the gathers were passed through a 10-20Hz Ormsby highpass filter followed by a 500ms AGC. Results for all components in groups 1, 2 and 3 are displayed in Figures 3, 4, and 5 respectively (the rectangular trace windows plotted on the gathers are discussed in the next section). On all vertical channels, high-frequency events between 500 and 1100ms displaying hyperbolic moveout are P-P reflections corresponding approximately to the Bow Island to Elk Point formations. The P-P reflections have a similar appearance at all geophone depths. P-wave reflections can be observed to arrive progressively later between the deepest and surface geophones (uphole interval velocities based on this time delay are discussed in a later section). The large gap in records from group 3 correspond to areas in the gathers where reflected data uncontaminated by ground roll are expected to occur.

The radial and transverse channels are, on the whole, relatively uncontaminated by P-P mode leakage. There is moderate P-P leakage on the radial channels at the 6 and 10m depth geophones of group 2, but these can be observed not to interfere with later P-S events. For reasons not completely clear, there is generally more P-P mode leakage on the transverse channel than the radial channel.

The hyperbolic low-frequency events at mid- to far-offsets from about 900 to 2000ms are converted-wave reflections corresponding approximately to the Second White Specs to Mississippian formations. Statics of 50-75ms can be observed in these gathers, especially in group 1, giving the hyperbolae a bumpy appearance in places. There is, overall, more converted-wave energy on the radial channels than the transverse, and so the frequency analysis (next section) was performed on the radial channels. As with the P-wave reflections, the converted-wave reflections appear very similar for geophones placed at different depths.

Frequency Analysis: Raw Data

Regions in the common receiver gathers that are relatively uncontaminated by ground roll and refracted arrivals occur between times of 700 and 1600 ms at mid- to far-offsets. It was in these areas of the receiver gathers that windows were chosen for frequency analyses, as they contained relatively noise-free reflections. Analysis windows for the raw data are outlined by the gray boxes in Figures 3, 4 and 5. The window times correspond approximately to reflections from the Mannville to Elk Point formations. These occurred between 700 and 1100 ms for the P-P reflections, and about 1000 to 1600 ms for P-S reflections. As mentioned previously, group 3 had broad no-shoot zones through areas expected to contain P-S reflections uncontaminated with coherent noise, so only a narrow strip of far-offset traces was analyzed for the radial channel of these gathers.

The frequency analysis was performed in Matlab using a program developed by CREWES (Margrave, unpublished), as this program permitted a high degree of versatility in the selection of analysis windows. Results of the frequency analysis of these time windows for the raw (non-gained, unfiltered) receiver gathers appear in Figure 6. The frequency spectra for the vertical and radial channels at all geophone depths are plotted on a vertical scale representing decibels down from maximum amplitude.

The P-P reflections have a signal width between about 10 and 45 Hz, with strongest amplitudes between 15 and 30 Hz. There is a notching pattern that is fairly consistent between the vertical channels in each group, but not between groups. These notches are likely due to near-surface reverberations (ghosting). As expected, there is no

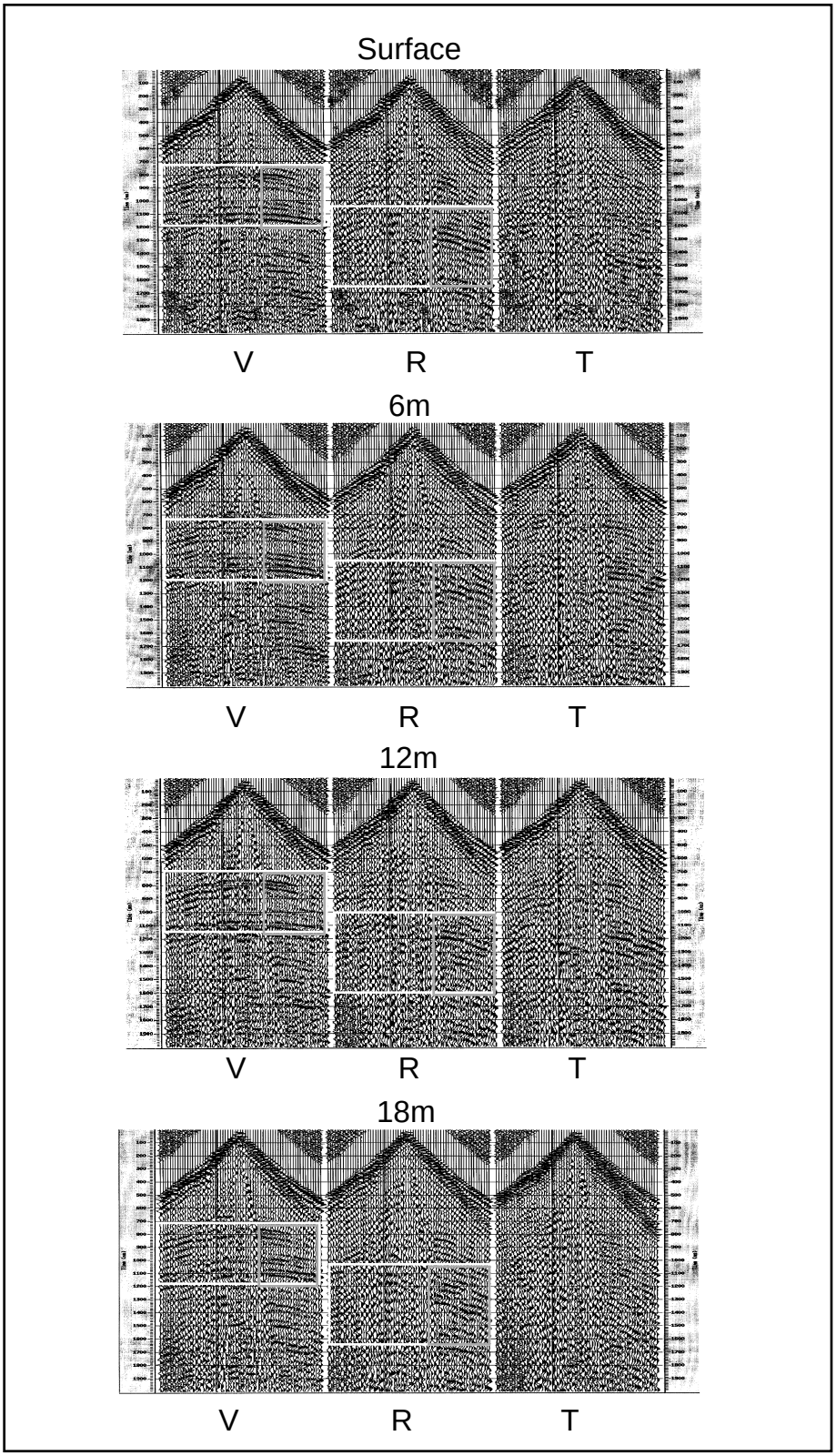

Figure 3. Group 1 receiver gathers, all channels. Data have been filtered to suppress ground roll and gained with a 500ms AGC. Trace windows represent data analysis locations (see text for details)

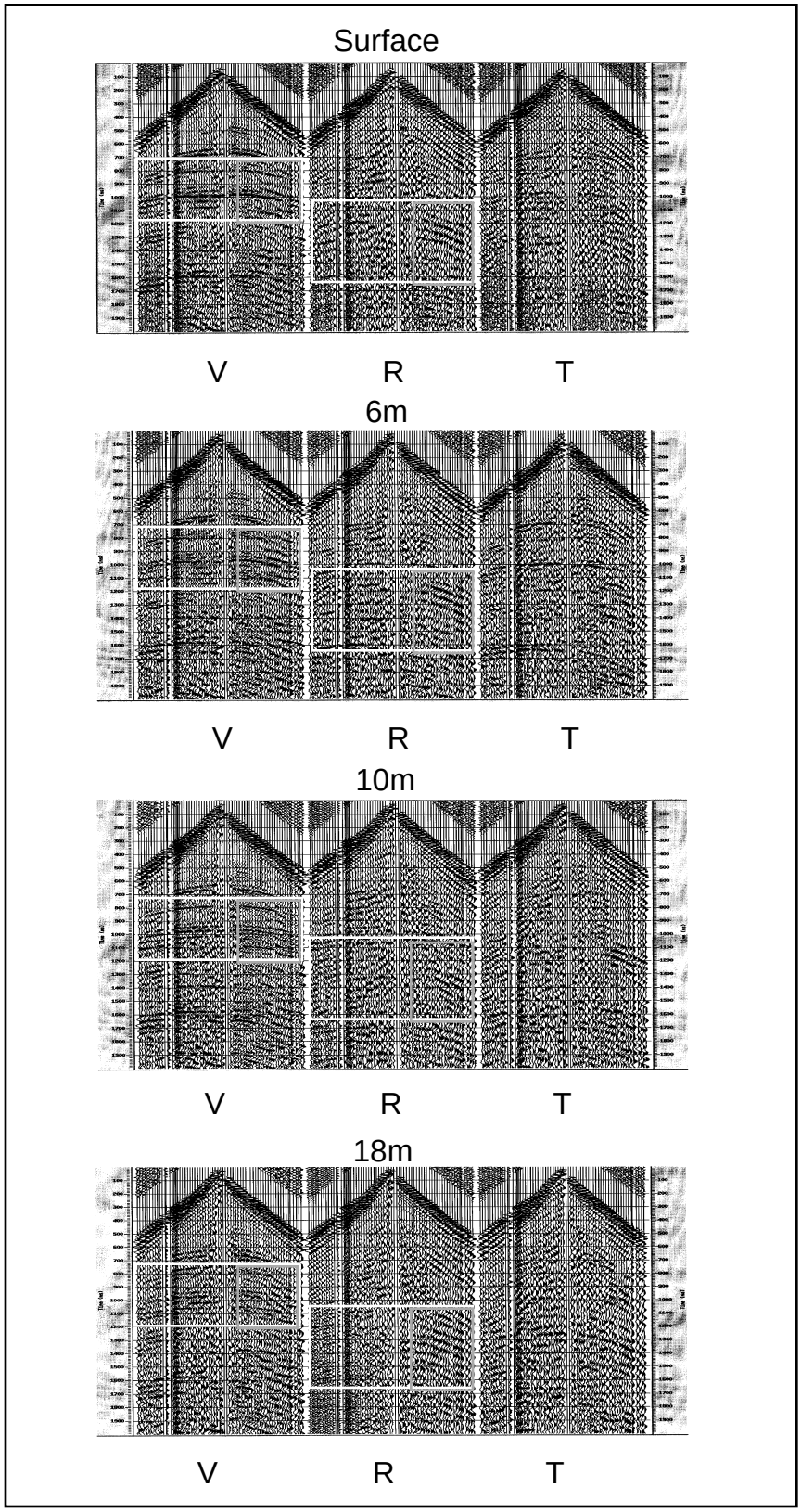

Figure 4. Group 2 receiver gathers, all channels. Data have been filtered to suppress ground roll and gained with a 500ms AGC. Trace windows represent data analysis locations (see text for details)

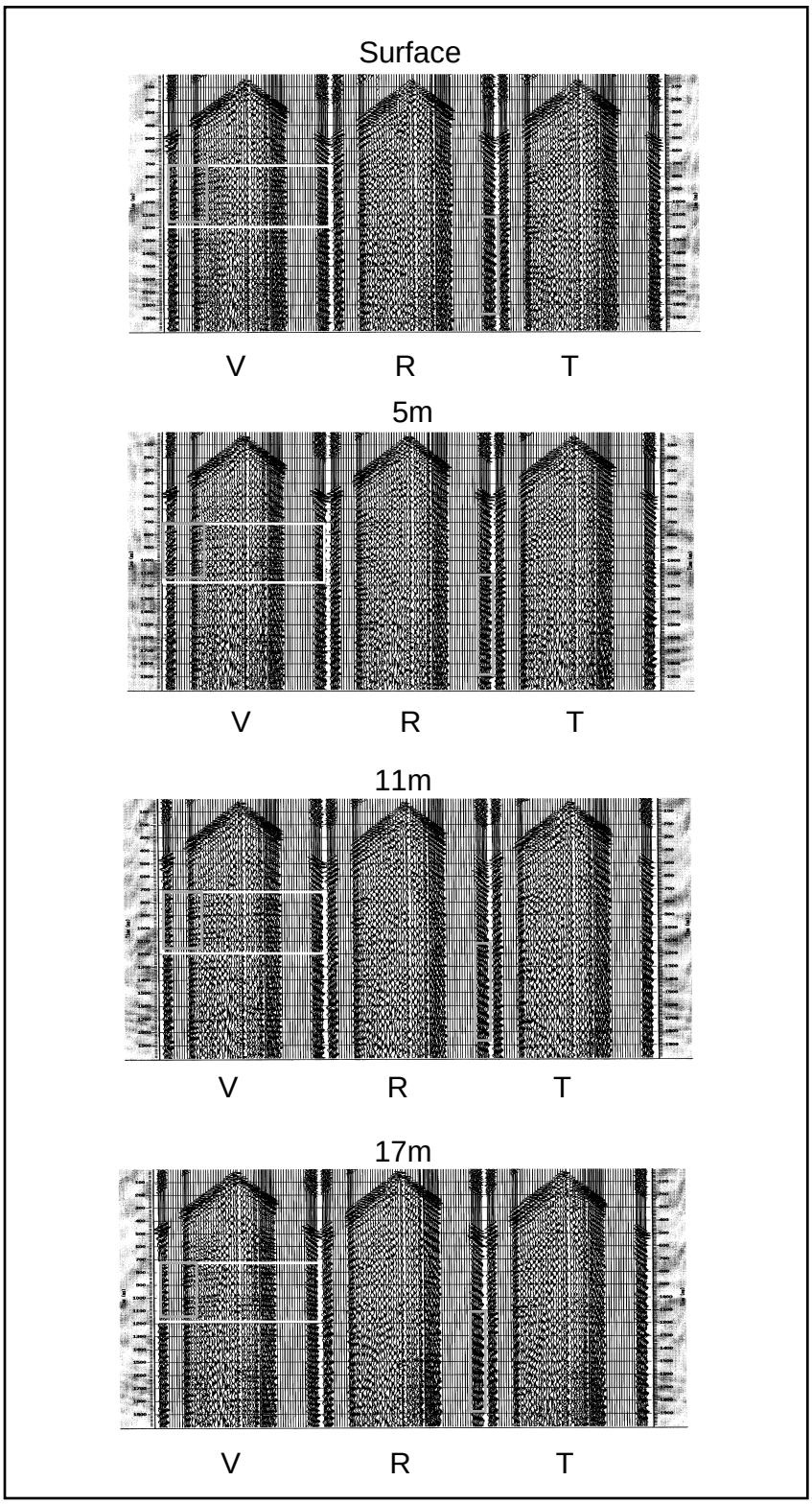

Figure 5. Group 3 receiver gathers, all channels. Data have been filtered to suppress ground roll and gained with a 500ms AGC. Trace windows represent data analysis locations (see text for details)

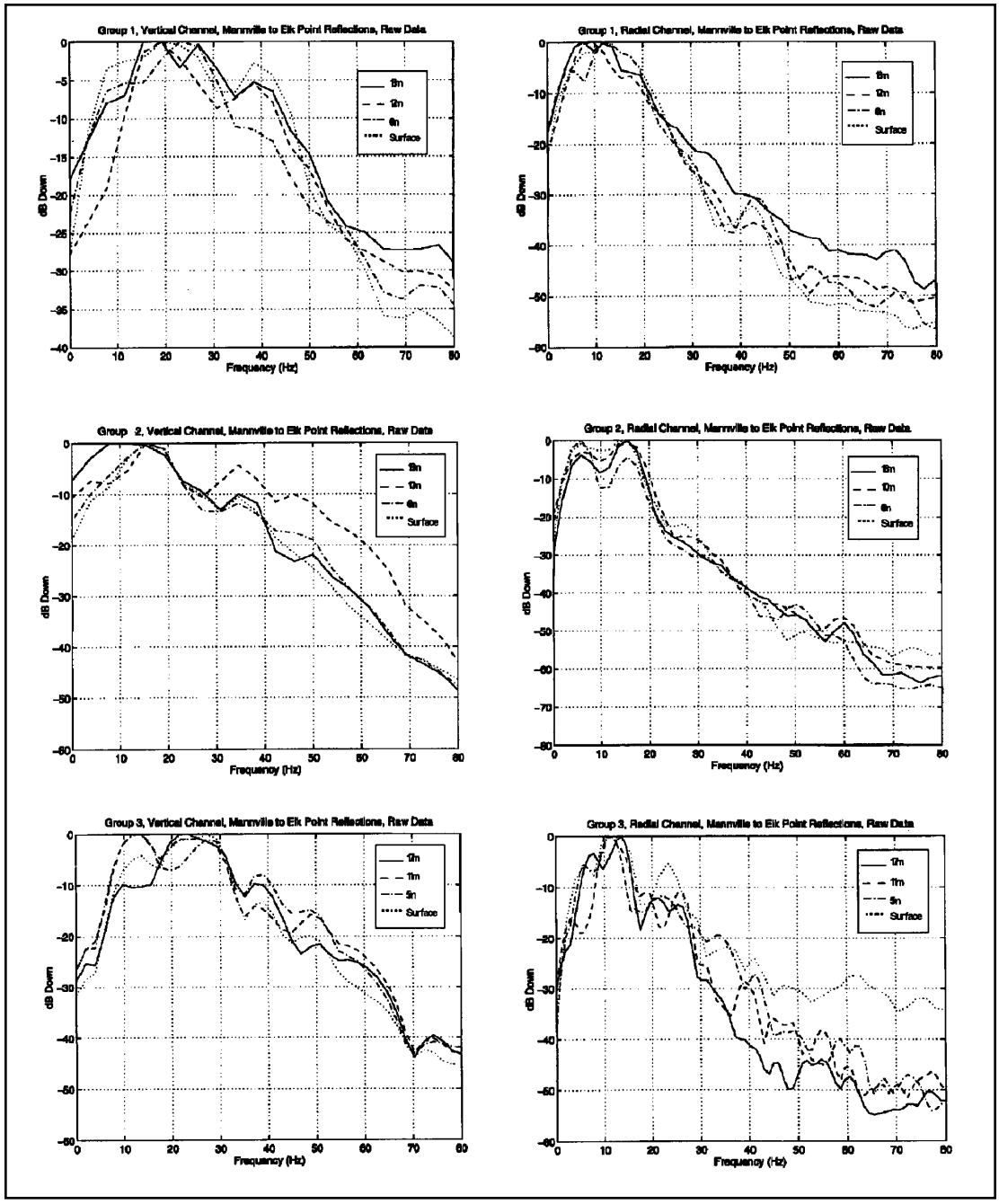

Figure 6. Frequency spectra of raw P-P and P-S reflections, for all groups.

evident trend of additional loss of high frequency signal between the deepest and surface geophones, demonstrating a lack of P-wave attenuation across the interval.

The amplitude spectra of the raw P-S reflections, also shown in Figure 6, have a much lower and narrower bandwidth than the P-P reflections, as has been observed for most other 3-C surface seismic data (e.g., Zhang et al., 1994). The P-S reflections are, therefore, at all depths, more attenuated than the P-P reflections. There are two fairly consistent peaks at 5-7 Hz and 12-16 Hz in the spectra. The lower peak is due to some ground roll noise captured in the analysis window; the higher frequency peak is from

P-S reflections. As with the P-P reflections, no apparent difference in attenuation between the different depths is evident.

Bandpass Filtered Data

The data were passed through a 10-20 Hz Ormsby highpass filter to reduce the ground roll noise observed in the frequency spectra of the raw radial data. The windows selected for frequency analysis were expanded to include all offsets for vertical channel data (the white rectangles in Figures 3, 4 and 5), but remained at mid- to far-offsets for the radial channels (the gray rectangles). Results are plotted in Figure 7. As with the vertical channel raw data, the high-passed data do not indicate attenuation between the deepest geophone depth and the surface. The high-passed radial channel, with ground roll noise in the stop band, shows that P-S reflections are confined mostly to the 10-22 Hz range. With the ground roll suppressed, the data are normalized to the maximum amplitude of the P-S reflections (as opposed to the ground roll), and no differential attenuation is evident between the different depths.

Many other filters with different passbands were tested, but no variation in shear-wave attenuation between the different depths was found.

f-k Filtered Data

To reduce coherent noise, the data were passed through an f-k filter polygon designed to reject ground roll and refracted arrivals. The f-k filter had dimensions 2000ms $\times$ 45 traces, with a value of 95% used for time ramp flattening, offset ramp flattening and f-k filter windowing. Figure 8 shows the f-k filtered output for the radial channel of the group 1, 6m depth geophone and the vertical channel of the group 2, 18m depth geophone. In these examples, the filter has effectively isolated the P-P and P-S reflections. The window for frequency analysis on the vertical channel included all offsets (the white rectangles), as reflections were observed to be fairly strong across the entire gather. The analysis window for the radial channels again remained confined to mid to far-offsets (the gray rectangles), due to the absence of signal at near offsets. This lack of signal near the center of the radial receiver gathers was due to the lower amplitude of P-S mode conversions at small angles of incidence.

The frequency spectra of the f-k filtered gathers appear in Figure 9. As before, vertical channels have a comparable bandwidth at all depths, with no evidence of differential attenuation. The radial channels show that the converted-wave reflections have a narrow 10-20 Hz bandwidth, and again no evidence of shear-wave attenuation appears.

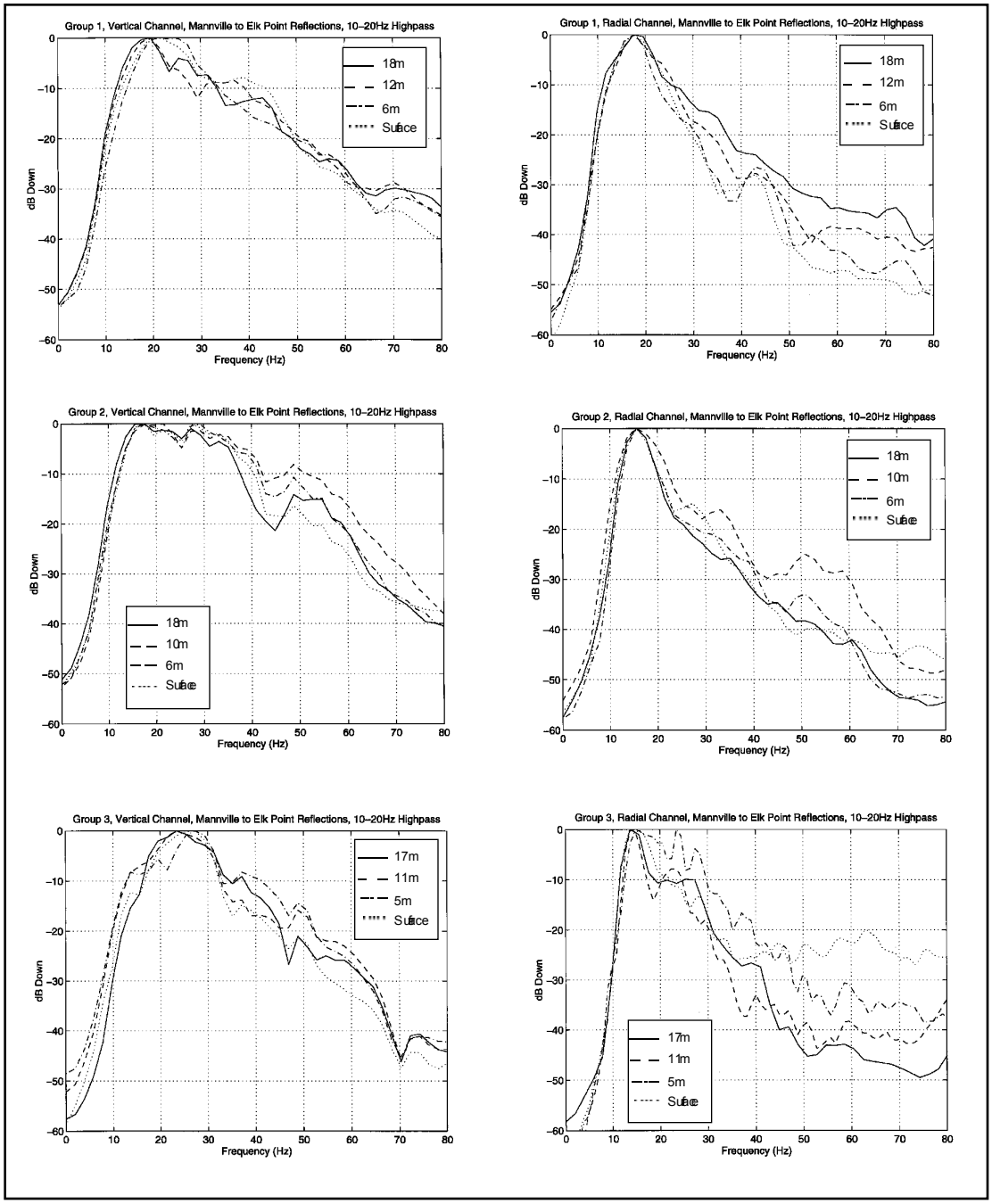

Figure 7. Frequency spectra of 10-20Hz high-passed P-P and P-S reflections.

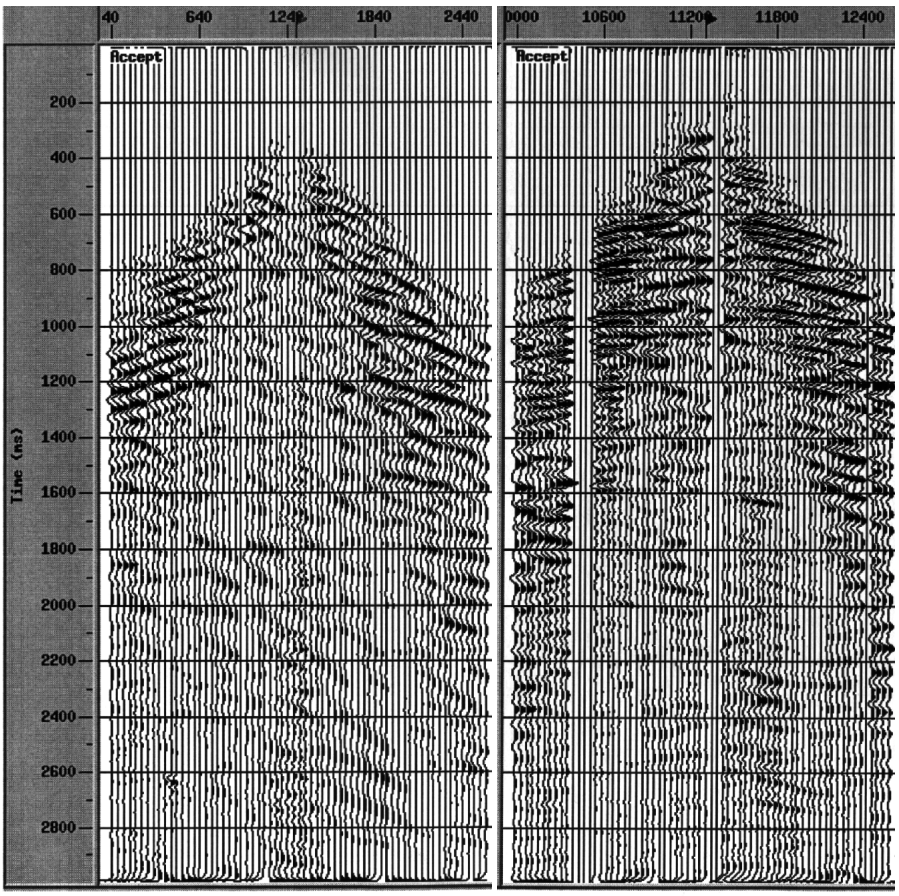

Figure 8. f-k filtered gathers from (a) group 1, radial channel, 6m depth, and (b) group 2, vertical channel, 18m depth.

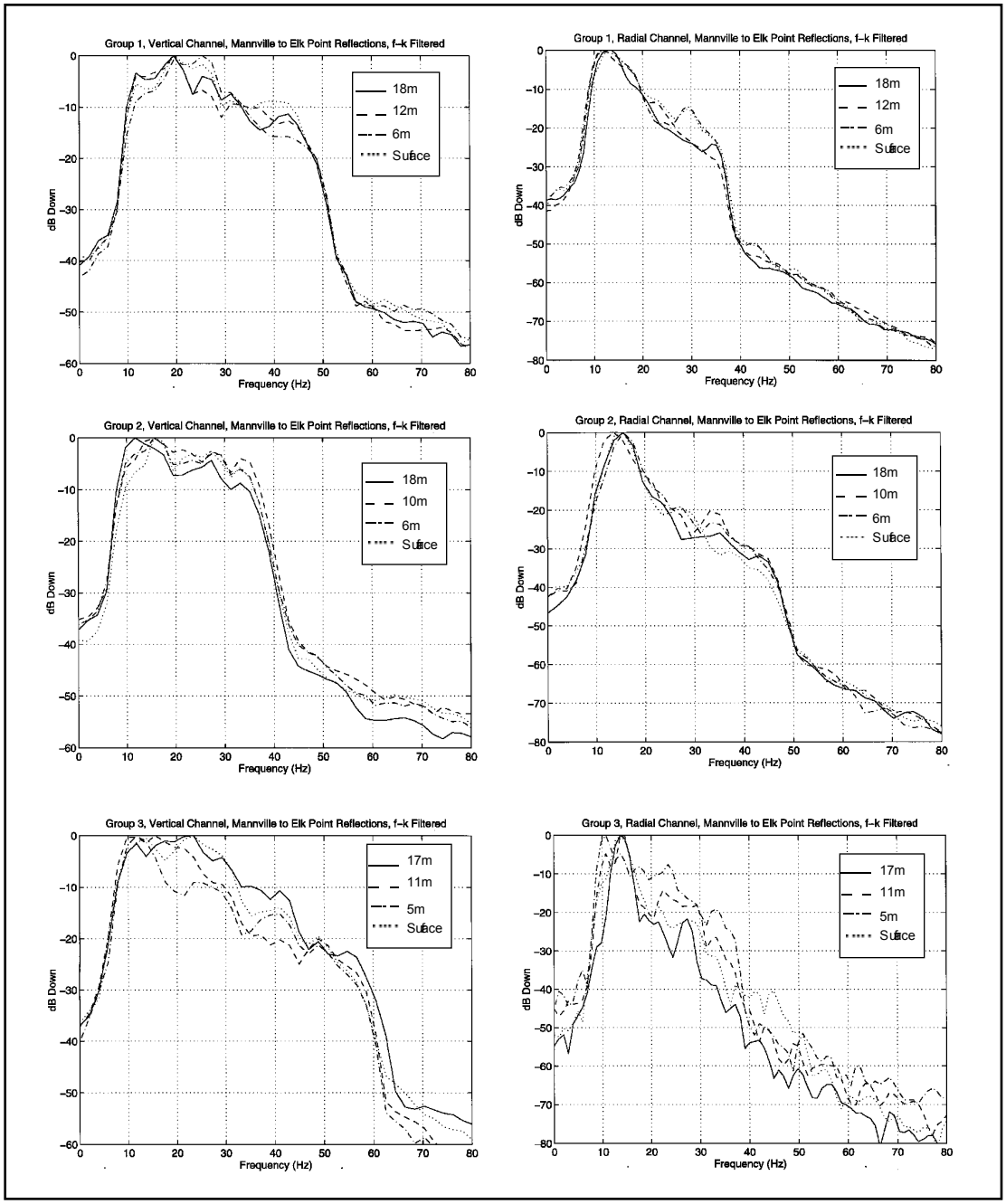

Figure 9. Frequency spectra of f-k filtered P-P and P-S reflections.

UPHOLE INTERVAL VELOCITIES

With the experimental setup, it is possible to directly calculate the P- and S-wave interval velocity of the overburden between any two geophone depths in the same group, assuming the reflection ascends vertically through the low-velocity layer. The ascending reflections will reach successively shallower geophones at progressively later times; hence, since the depths of the geophones are known and the arrival times are recorded in the traces, the interval velocities can be calculated directly.

To determine interval lag times, a Matlab computer function was written that performs a trace-to-trace cross-correlation between two receiver gathers. The function cross-correlates each trace in a receiver gather with the corresponding trace (i.e. the one with the same shot number) in the same channel but for a different geophone depth. The user inputs the time windows in each trace to correlate and the number of lags to correlate. The time window is chosen so as to contain as many clear, coherent reflections as possible across the gather. This corresponded to areas outlined by the white rectangles in Figures 3, 4 and 5. The program determines the time lag of maximum (positive) correlation to the nearest tenth of a sample, using cubic spline interpolation, between each trace in the gathers being compared.

The appropriate number of lags to correlate is determined iteratively by examining the output of the program. The lag is increased if the point of maximum correlation between the traces is low, and decreased if lag times are inconsistent across the gather. Results are saved to user-specified variables and then displayed graphically. The technique works best on f-k filtered data, because the f-k filter suppresses coherent noise that tends to correlate between traces, but generally only for large lag times.

Figure 10 shows the program output for four intervals in the vertical channel of group 1. Figure 10(a) shows that the maximum correlation is generally above 0.4 for mid- to far offsets, and falls below this for near offsets (in the center of the gather). The center of the gather was largely contaminated with ground roll prior to f-k filtering, as discussed in the previous section, which caused this poor correlation.

Figure 10(b) shows the time lag at which maximum correlation occurred. Lags are, overall, fairly consistent across the entire gather, indicating that correlation is being made based on coherent reflections. The exceptions occur in the middle of the gather, where there is poor correlation. The 18m to 0m lag is included as a test of the robustness of the technique; the three interval lag times between 18m and 0m should sum to the total lag time from 18m to 0m. The difference between the sum of the average interval lag times and the total lag time (excluding traces from the center of the gather) is only 1.3ms, indicating that, for this group, interval times are being determined with a fairly high accuracy.

This plot clearly demonstrates the dramatic P-wave velocity change over the top 18m of the low-velocity layer. The average time lag between the 18m and 12m depth is 2.5 ms, for a P-wave interval velocity of about 2400 m/s. The 12m to 6m interval has a time lag of about 10.5 ms, giving an interval velocity of 570 m/s, and the 6m to 0m interval has a time lag of about 19.5 ms, giving an interval velocity of about 310 m/s. The large drop in velocity between the two lowest intervals is probably due to the water table. Lawton (1990) found similar results for a refraction survey near Jumping Pound, Alberta.

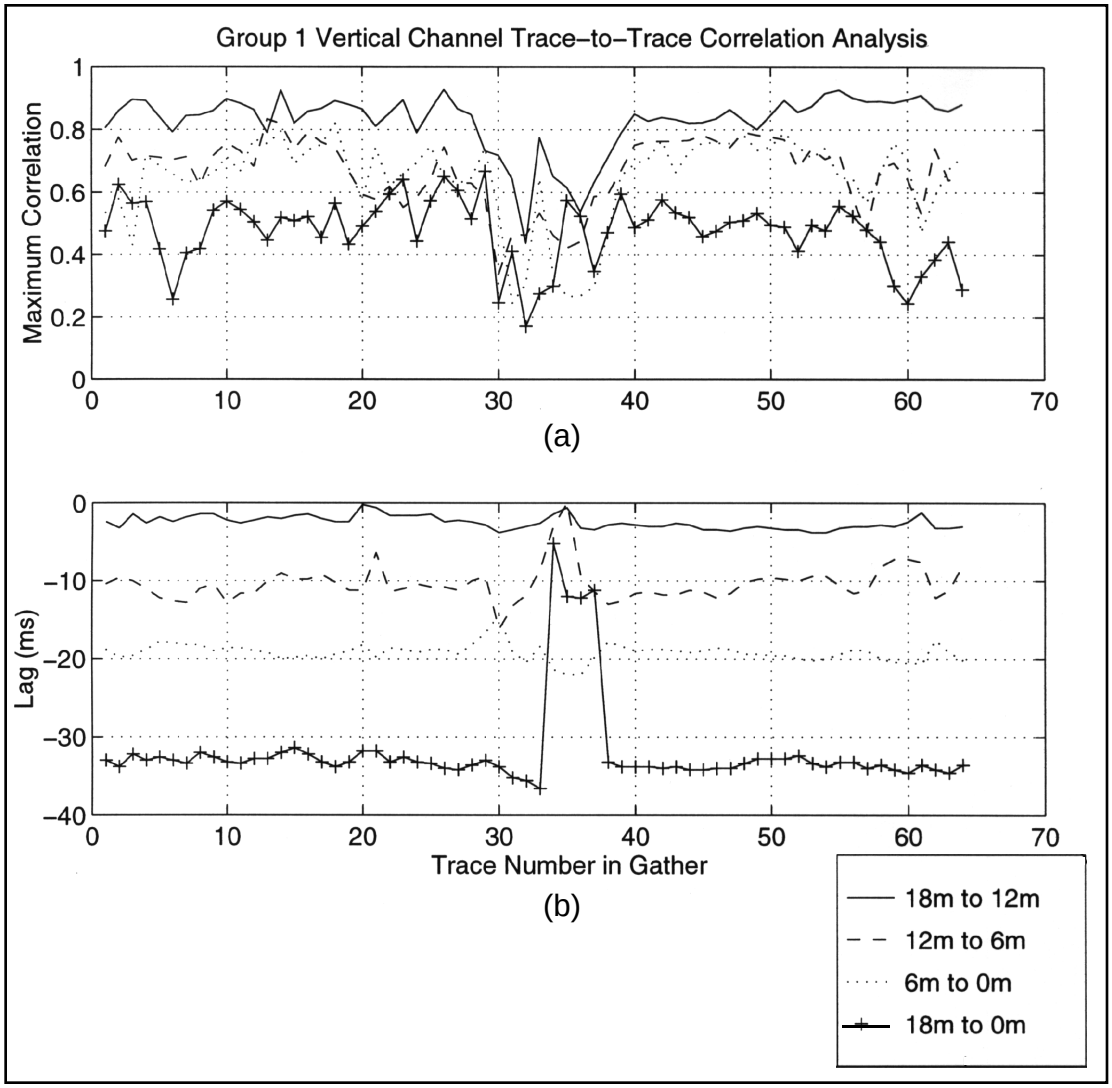

Figure 10. (a) Maximum correlation values between selected geophone intervals of group 1, P-P reflections. (b) The lag time at point of maximum correlation.

Figure 11 shows the same cross-correlation analysis for the radial channels of group 1. The maximum correlation coefficients (Figure 11(a)) are lower and much less consistent between traces of the radial channel than the vertical channel. The lag times (Figure 11(b)) are also less consistent between traces, at all source-receiver offsets. This low coherence between converted-wave reflections at different levels is due to low signal-to-noise ratios, caused by the relatively low amplitudes of the converted-wave reflection. Due to these greater noise levels, only certain intervals had sufficiently consistent trace-to-trace lags to permit a reasonably confident interval time. For example, in Figure 11(b), the 6m to 0m interval lag times are relatively consistent between trace numbers 1 and 27 and 36 and 64. The mean lag of these intervals is -34.7 ms, which was used to calculate interval velocities. Possibly due to high noise levels, the 18m to 12m interval lag times were not consistent across any significant portion of the gather, and so were not used in calculating an interval velocity. Due to such uncertainties in shear-wave lag times, shear-wave velocities could not be calculated for most intervals. No confident interval velocities could be calculated at all for group 3 shear-waves, probably due to the large “no shoot” zones that should have contained

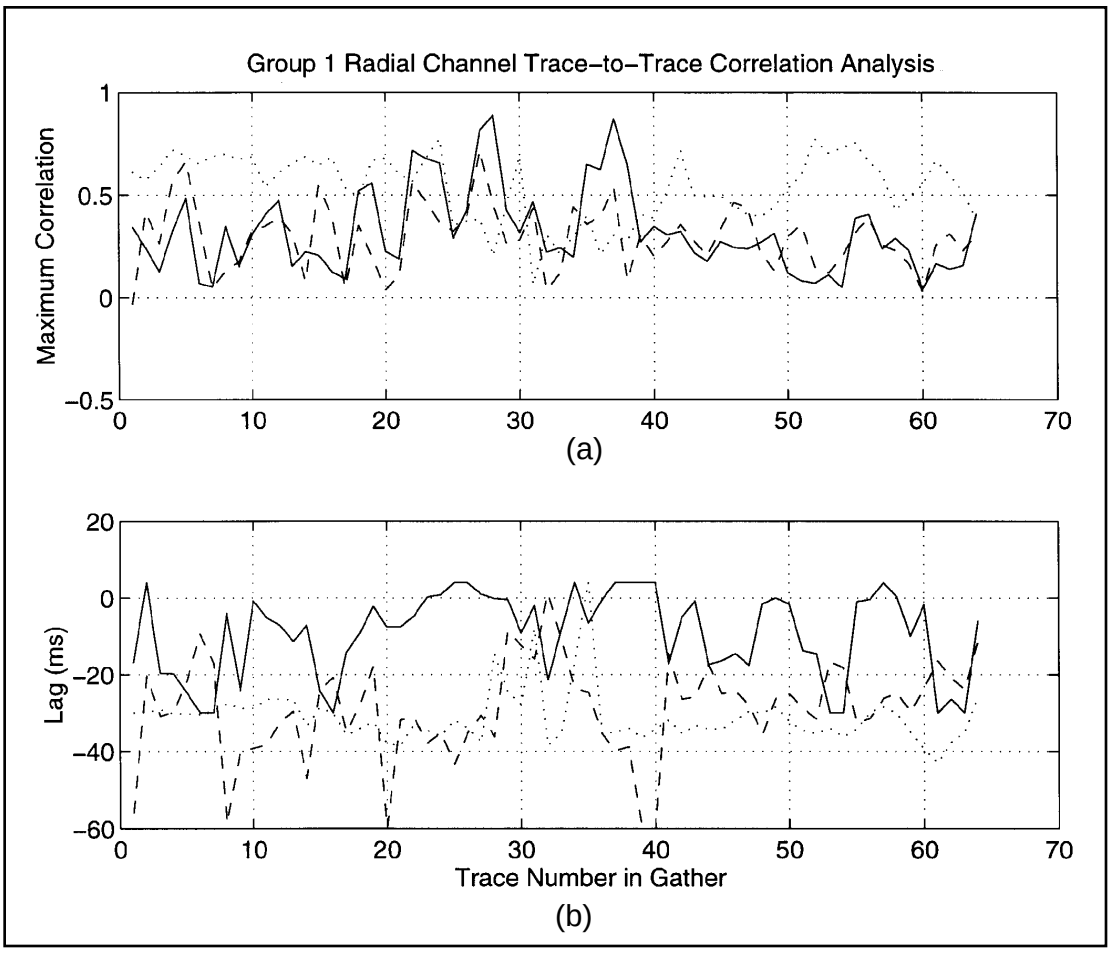

Figure 11. (a) Maximum correlation values between selected geophone intervals of group 1, P-S reflections. (b) The lag time at point of maximum correlation. Legend same as Figure 10.

low-noise converted-wave reflections. Results of receiver gather correlation analysis for the other two groups are shown in Figures 12, 13 and 14.

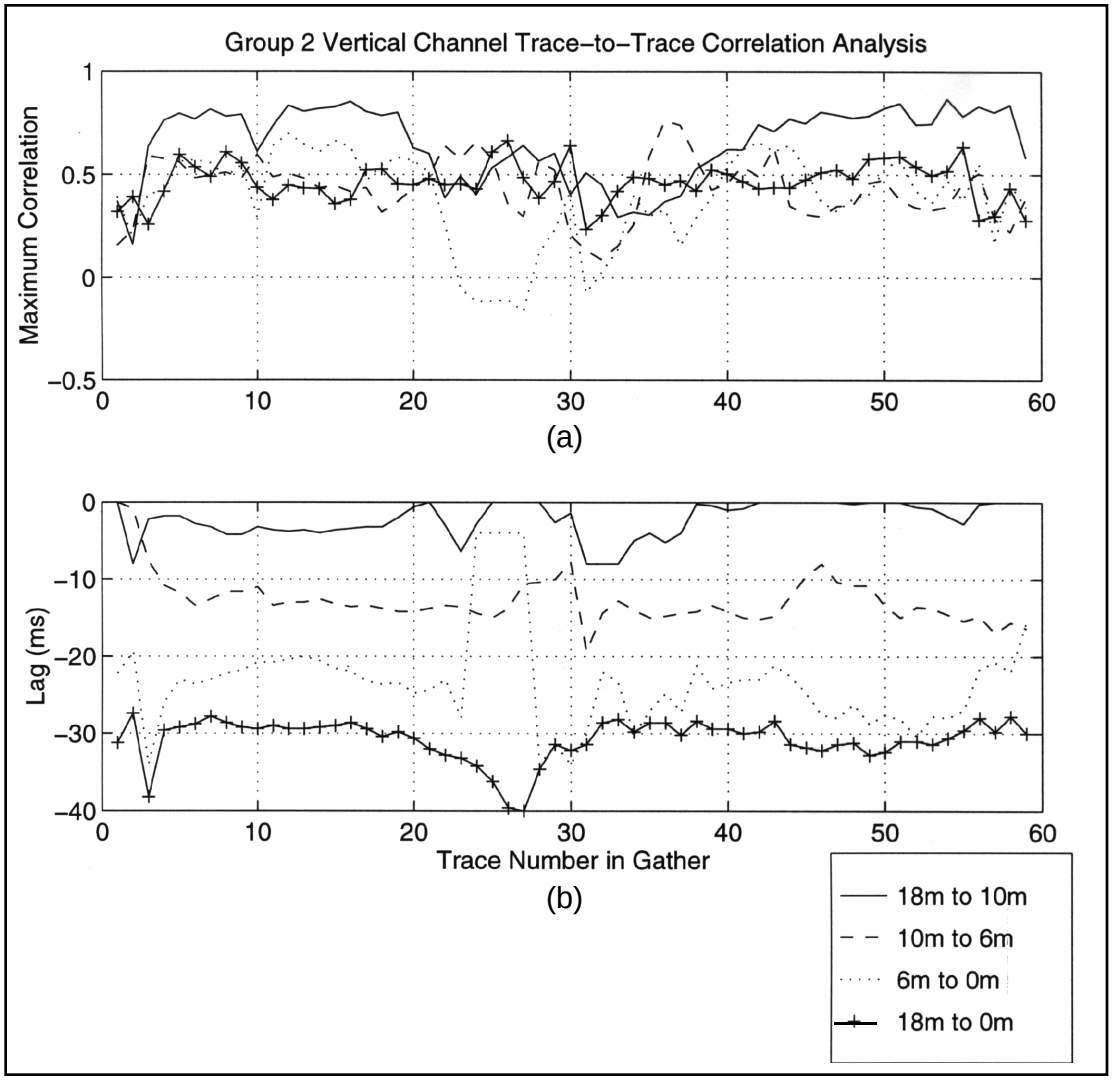

Figure 12: (a) Maximum correlation values between selected geophone intervals of group 2, P-P reflections. (b) The lag time at point of maximum correlation.

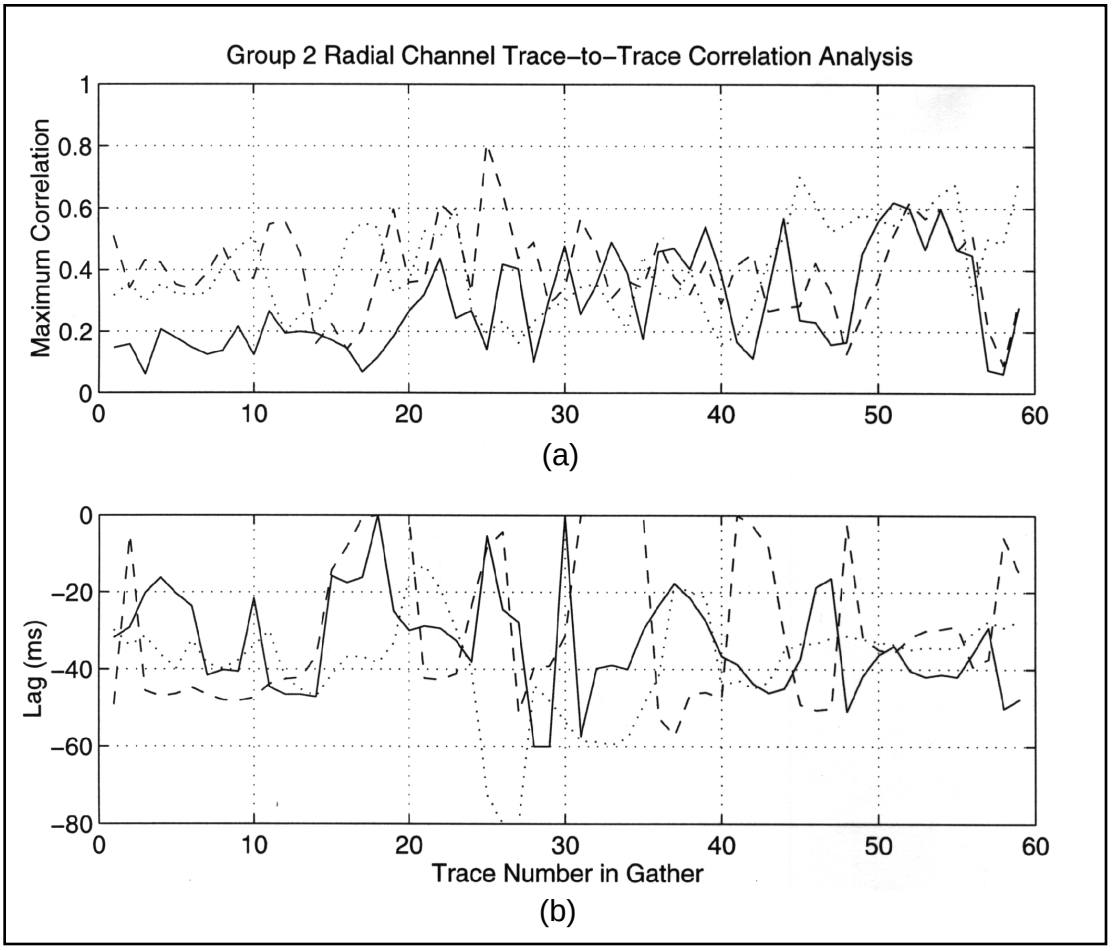

Figure 13. (a) Maximum correlation values between selected geophone intervals of group 2, P-S reflections. (b) The lag time at point of maximum correlation. Legend same as Figure 12.

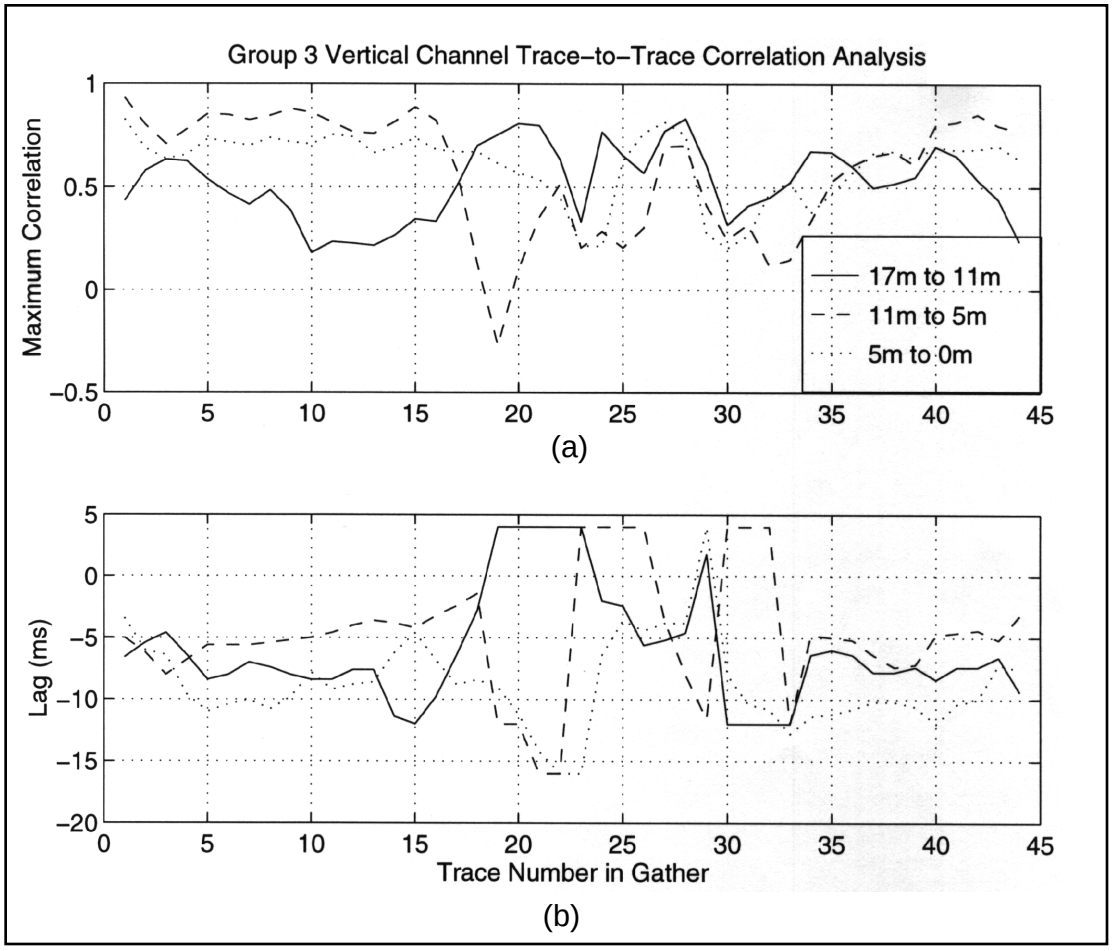

Figure 14. (a) Maximum correlation values between selected geophone intervals of group 3, P-P reflections. (b) The lag time at point of maximum correlation.

Figure 15 shows schematically the P and S-wave velocities between every interval it could be confidently calculated, for all three groups. Where both interval P and S-wave velocities have been determined, the Vp/Vs ratio for that interval is given in the left-hand column.

The results show that S-wave velocity falls in the 150-300 m/s range expected of unconsolidated sediment, and increases slightly with depth. The comparison of the lowest to middle interval of group 2 demonstrates that shear-wave velocity is not affected by the water table, while P-wave velocity is far greater below the water table than above. Again these results are corroborated by a refraction survey (Lawton, 1990). This great difference between P-wave and S-wave velocities in saturated overburden results in an extreme Vp/Vs of 10.7 for the 18m to 10m interval of group 2. Probably due to lack of good reflections, interval velocities of group 3 are inconsistent and no water table is indicated.

The extreme Vp/Vs implies that S-waves in saturated overburden have a wavelength about a tenth that of P-waves of the same frequency. As attenuation for a wave is proportional to the number of cycles it completes, shear-waves would be expected to attenuate much faster in a saturated overburden layer than compressional waves of the same frequency, assuming an approximately equivalent attenuation constant for each type of wave. A thick but mostly saturated overburden layer would account for the

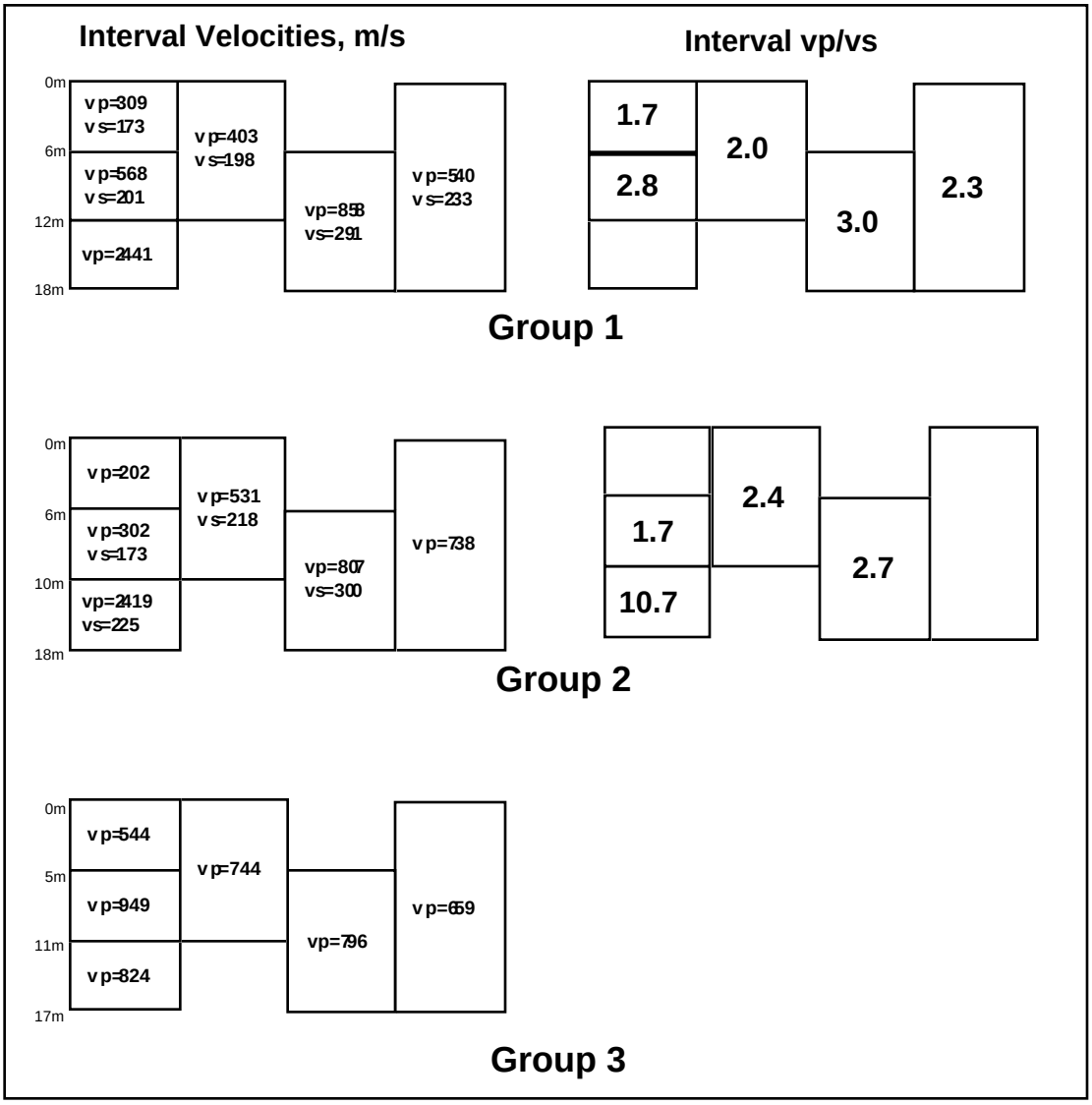

Figure 15: Uphole interval velocities for all groups, and Vp/Vs for intervals where both Vp and Vs could be determined.

much greater attenuation seen in the converted-wave than the P-P-wave in the receiver gathers.

A three-layer weathering layer model was obtained from the company that processed the 2-D line data. This model was based on a multi-layer P-wave refraction analysis. Layer 1 can be interpreted as "unsaturated overburden", has a P-wave velocity of 610 m/s, layer 2 is "saturated overburden" which has a velocity of 2184 m/s, and layer 3 is considered the top of the bedrock, with a velocity of 2827 m/s. The model agrees with observations from uphole interval times in broad terms only, for groups 1 and 2. A water table depth of 10m for group 2 is indicated by both the model and uphole interval velocities from the buried geophones. The model indicates an absence of saturated overburden for group 1, whereas P-wave interval velocities suggest the presence of a water table between 12 and 18m.

CONCLUSIONS

The P-P reflection bandwidth was about 15-45 Hz at all geophone depths, with no differential attenuation evident through the top 18m of overburden. The P-S reflection bandwidth was considerably attenuated at all depths compared to the P-P reflections, with dominant frequencies between 10 and 22 Hz, even at 18m below the surface. The frequency spectra of the converted-wave reflections (raw and filtered) at all depths for all groups do not vary systematically with depth. It can be concluded, then, that *converted-wave reflections are already severely attenuated at a depth of 18m in the study area, and that no significant additional attenuation is suffered by the reflections as they pass through the top 18m of the overburden layer.* Lack of attenuation through the top 18m of overburden was also noted for the P-P reflections.

Uphole interval velocity times indicate a water table depth of 10 to 12m, as indicated by the significant increase in P-wave velocities below this depth. S-wave velocities are unaffected by the water table, remaining low both above and below it. This implies that they have a much shorter wavelength than P-waves of a similar frequency below the water table. This might account for the much greater attenuation seen in the P-S reflections than the P-P reflections.

RECOMMENDATIONS

This experiment would probably successfully detect shear-wave attenuation in the low-velocity layer if the geophones are buried deeper and separated by larger intervals. Ideally, the deepest geophone should sit directly on the top of the bedrock, with succeeding geophones spaced evenly to the surface. This should provide fairly detailed information on the shear-wave attenuation properties of the low-velocity layer.

Fitting the geophones with high strength cable is recommended to make recovery of these expensive phones possible.

ACKNOWLEDGMENTS

We would like to thank our sponsor for their tremendous assistance in this study, and Mr. Eric Gallant who conducted most of the field operations. Also, thanks to Dr. Gary Margrave for his helpful suggestions.

REFERENCES

Geis, W.T., Stewart, R.R., Jones, M.J., and Katopodis, P.E., 1990. Processing, correlating, and interpreting converted shear-waves from borehole data in southern Alberta: Geophysics, **55**, 660-669.

Lawton, D.C., 1990. A 9-component refraction seismic experiment: Canadian Journal of Exploration Geophysics **26**, 7-16.

Margrave, G.F., unpublished. Seismic signal band estimation using f-x spectra.

Toksöz, M.N, Johnston, D.H., and Timur, A. Attenuation of seismic waves in dry and saturated rocks: I. Laboratory measurements. Geophysics, **44**, 681-690.

Westgate, J.A., 1963. Surficial geology of Foremost-Cypress Hills, 1:250000, Research Council of Alberta Bulletin 22.

Zhang, Q., San, Z., Brown, R.J. and Stewart, R.R., 1994. VSP interpretation from Joffre, Alberta. CREWES Research Report **6**, Ch. 33.